Short communication

Direct ammonia solid oxide fuel cell based on thin proton-conducting electrolyte

Limin Zhang, Weishen Yang *

State Key Laboratory of Catalysis, Dalian Institute of Chemical Physics, Chinese Academy of Sciences, Dalian 116023, China

Abstract

Thin proton-conducting electrolyte with composition $BaCe_{0.8}Gd_{0.2}O_{3-\delta}$ (BCGO) was prepared over substrates composed of $Ce_{0.8}Gd_{0.2}O_{1.9}$ (CGO)-Ni by the dry-pressing method. Solid oxide fuel cells (SOFCs) were fabricated with the structure $Ni-CGO/BCGO/Ba_{0.5}Sr_{0.5}Co_{0.8}Fe_{0.2}O_{3-\delta}$ (BSCFO)-CGO. The performance of a single cell was tested at 600 and 650 °C, with ammonia directly used as fuel. The open circuit voltages (OCVs) were 1.12 and 1.1 V at 600 and 650 °C, respectively. The higher OCV may be due to both the compaction of the BCGO electrolyte (no porosity) and complete decomposition of ammonia. The maximum power density was 147 mW cm^{-2} at 600 °C. Comparisons of the cell with hydrogen as fuel indicate that ammonia can be treated as a substitute liquid fuel for SOFCs based on a proton-conducting solid electrolyte.
© 2007 Elsevier B.V. All rights reserved.

Keywords: Solid oxide fuel cell; Ammonia; Proton-conducting solid electrolyte; Thin-film electrolyte

1. Introduction

To reduce dependence on fossil fuels, diversify renewable and sustainable energy sources and reduce pollution and greenhouse gas emissions, fuel cells have been extensively investigated as a clean and efficient power generation system. Of the various fuel cell types, solid oxide fuel cells (SOFCs) combine the benefits of environmentally benign power generation with fuel flexibility [1]. Hydrogen is the preferred fuel, but hydrogen production, storage, and the refueling infrastructure still pose major challenges. In particular, for mobile systems such as cars, the need for efficient hydrogen storage strategies is evident. Ammonia is a good hydrogen carrier, and is carbon free. It can be easily liquefied under about 10 atm at ambient temperature or at −33 °C under atmospheric pressure, it can be stored easily and is widely available [2]. Ammonia, although well known as a feedstock for producing hydrogen [3], has received little consideration for use as a direct fuel for SOFC [4–9].

While SOFCs based on an oxygen-ion conducting electrolyte, such as YSZ, are already in a mature state after

several decades of development, NO$_x$ may be produced in the direct ammonia conventional SOFCs [10,11]. High-temperature proton conductors have also been studied as a promising alternative electrolyte for intermediate or lower temperature SOFCs because of their low activation energy for proton conduction [12–15]. Moreover, pure proton conductors provide the possibility of fuller utilization of the fuel, as there is no water handling or dilution of the fuel [16,17]. Many perovskite-type oxides show high proton conductivity in a reducing atmosphere [18–21]. For example, doped barium cerate (BaCeO$_3$) materials have sufficiently high ionic conductivity over the wide temperature range of 300–1000 °C. To fuel SOFCs based on a proton-conducting electrolyte (such as doped-BaCeO$_3$) with ammonia is an effective way to avoid formation of NO$_x$. At the anode, ammonia is cracked to produce hydrogen and nitrogen, protons are generated at the anode and transported through the proton-conducting electrolyte to the cathode where they react with surface oxygen ions generated electrochemically from oxygen. Overall, nitrogen and water are the only chemical products of the direct ammonia fuel cell utilizing a proton-conducting solid electrolyte.

In this paper, SOFCs have been developed based on a Gd-doped-BaCeO$_3$ BaCe$_{0.8}$Gd$_{0.2}$O$_{3-\delta}$ (BCGO) thin film and the cell performance has been reported with commercial ammo-

* Corresponding author. Tel.: +86 411 84379073; fax: +86 411 84694447.
 E-mail address: yangws@dicp.ac.cn (W. Yang).

nia as fuel and oxygen as oxidant operating at temperatures of 600–650 °C.

2. Experimental

Doped barium cerate ($BaCe_{0.8}Gd_{0.2}O_{3-\delta}$) and $Gd_{0.2}Ce_{0.8}O_{1.9}$ (CGO) powders were prepared by combined citrate and ethylenediaminetetraacetic acid (EDTA) complexing synthesis techniques with appropriate stoichiometric precursors of $BaCO_3$ (99%), CeO_2 (99.9%), and Gd_2O_3 (99.99%).

Instead of barium cerate, we selected CGO as the ceramic component for the substrate due to better sintering activity and mechanical properties. Commercial NiO (60 wt.%) and CGO (40 wt.%) powders were mixed and ground with alcohol for 2 h. After the alcohol had been evaporated, the dried mixture was first pressed under 100 MPa into a substrate in a stainless-steel die. Then, the BCGO powder was added and co-pressed at 200 MPa to form a green bilayer and subsequently co-fired at 1450 °C in air for 3 h to densify the BCGO film, and a dense, well-bonded electrolyte–anode assembly was obtained. The thickness of the BCGO layer was well controlled by the amount of powder added. The total thickness of the electrolyte–anode substrate assembly was about 1 mm. Graded cathodes were applied to optimize performance by printing. The first layer was $Ba_{0.5}Sr_{0.5}Co_{0.8}Fe_{0.2}O_{3-\delta}$ (BSCFO) 80 wt.%, CGO 20 wt.%, the second layer was pure BSCFO and then it was co-fired at 970 °C in ambient air for 5 h using heating and cooling rates of 120 °C h^{-1} to form a porous cathode. To minimize the contact resistance between the cathode and Ag mesh, Ag paste was painted on the cathode surface to serve as a current-collector. The assembly was then sintered at 600 °C for 30 min.

Cells were tested at 600 and 650 °C in a home-made system with commercial liquefied ammonia or humid hydrogen (∼3% H_2O) as fuel and oxygen as oxidant, respectively. Digital multi-meters (XIELI, DPM) were used to collect the voltage and current data for the cells. During cells operation, the inlet flow rate of NH_3 (H_2) to the anode was maintained at 30 cm^3 min^{-1}, and the flow rate of oxygen at the cathode was 50 cm^3 min^{-1}.

Phase identification of the BCGO powder and BCGO electrolyte film was studied with powder X-ray diffraction (XRD,
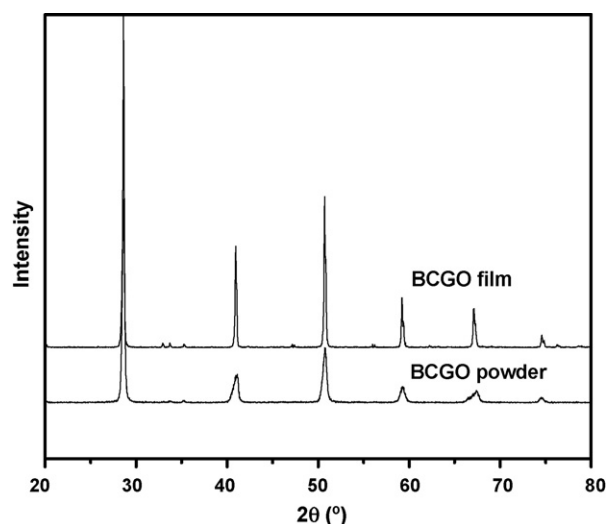

Fig. 1. XRD patterns of BCGO powder and a BCGO thin film.

Rigaku D/Max-RB) and using Cu Kα radiation. The microstructures of the sintered films and tested cells were characterized by scanning electron microscopy (SEM, FEI Quanta 200 FEG).

3. Results and discussion

3.1. Film characterization

The dry-pressing process is a simple, reproducible and cost-effective approach for thin-film fabrication [22]. Fig. 1 shows the X-ray diffraction patterns of an as-sintered BCGO film and the starting powder. The data show good phase purity in the BCGO film, and no other evident phases were detected. Fig. 2(a) shows a cross-sectional view of a post-test cell with Ni-CGO/BCGO/CGO-BSCFO. It was observed that the BCGO film was about 30 μm thick and uniform, and appeared well-bonded to the Ni-CGO substrate. It can be seen clearly in Fig. 2(b) that the as-sintered BCGO film is free from pores and cracks within the scale of SEM observation. These results indicate that the 30 μm thick BCGO electrolyte film has been successfully fabricated on the Ni-CGO substrate by the dry-pressing method.
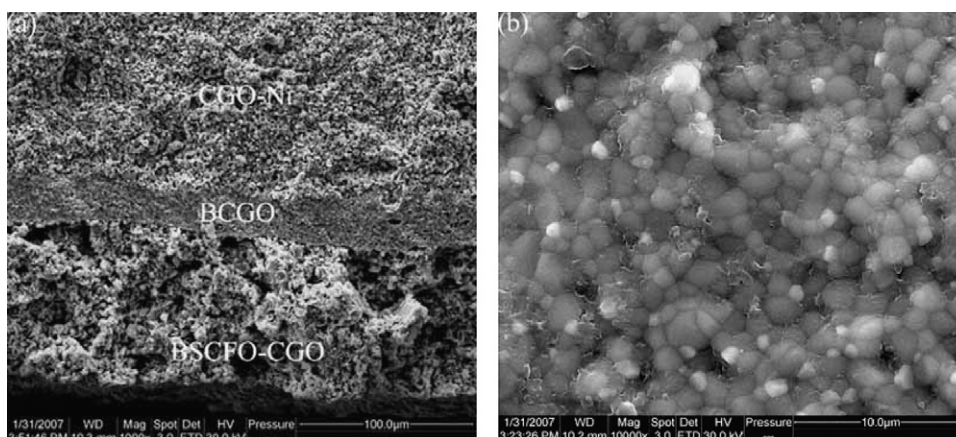

Fig. 2. SEM micrographs of a fracture surface of a post-test cell (a) and the as-sintered surface of BCGO film (b).
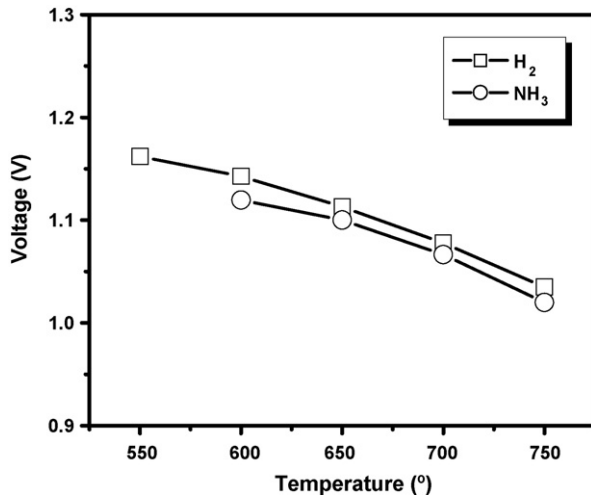
Fig. 3. OCVs of the cell with ammonia or hydrogen as fuel and oxygen as oxidant at different temperatures.

3.2. Fuel cell measurements

Fig. 3 shows the effect of increasing temperature on the open circuit voltage (OCV) of the same SOFC operating on ammonia and hydrogen, respectively. It can be seen that the OCVs essentially decrease with increasing temperature. The measured OCVs of a SOFC operating on ammonia were slightly lower than that on wet hydrogen. The reason can be attributed to a lower partial pressure of hydrogen due to the co-production of nitrogen. The OCVs were 1.14 and 1.12 V at 600 °C operating on wet hydrogen and ammonia, respectively, close to the theoretical value, indicating that a dense BCGO film had formed. However, as operating temperature increased to 750 °C, the OCVs were only 1.035 and 1.02 V fueled with wet hydrogen and ammonia, respectively, which were less than the theoretically expected values. The reason for the lower voltage was most probably due to electronic conductivity development on the BCGO electrolyte at higher temperature.

Fig. 4 shows I–V curves together with the power density of the cell fueled with ammonia. Relationship between the terminal
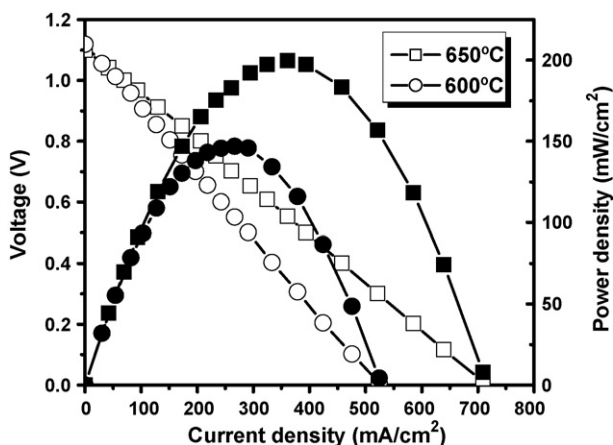

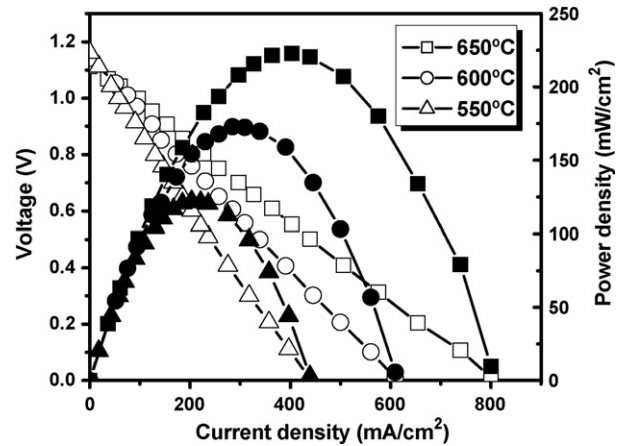Fig. 4. I–V characteristics of fuel cell with ammonia as fuel and oxygen as oxidant at different temperatures.

Fig. 5. I–V characteristics of fuel cell with wet hydrogen ($\sim$3% H_2O) as fuel and oxygen as oxidant at different temperatures.

voltage and the current density is linear, which demonstrates that the electrodes polarization is low due to the better compatibility between the electrolyte and the electrode materials, and the complete decomposition of the inlet NH_3 into H_2 and N_2 within the range of temperatures under investigation. A steady and stable current supplied by the cell indicates that the dense BCGO thin film could serve as the solid electrolyte of a fuel cell. With ammonia as fuel and oxygen as oxidant, maximum power densities of 147 and 200 mW cm^{-2} were obtained at 600 and 650 °C, respectively. At the peak power cell voltage of 0.55 V (about OCV/2), current density of 0.361 and 0.267 A cm^{-2} were measured at 650 and 600 °C, respectively. The power density decreases as temperature decreases because the cell resistance increases. In addition to the performance with ammonia as fuel, the same cell was also tested at 650 and 600 °C with wet hydrogen as fuel, and the results are shown in Fig. 5. With oxygen as oxidant, maximum power densities of 223 and 172 mW cm^{-2} were obtained at 650 and 600 °C, respectively. The maximum power densities were only slightly higher when the cell was operated using hydrogen compared to ammonia. Comparisons of the cell with hydrogen as fuel indicate that ammonia can be treated as a substitute liquid fuel for SOFCs based on a proton-conducting solid electrolyte.

The improved power output is attributed to the use of a thinner electrolyte. The long-term stability for electrolyte materials in the working environment is a major factor. Doped-$BaCeO_3$ has sufficiently high ionic conductivity at low temperatures, but the chemical stability in an atmosphere containing CO_2 and H_2O is a major challenge for fuel cell applications [23,24]. The long-term performance of cells with direct air oxidant will be investigated in later work.

4. Conclusions

A direct ammonia SOFC based on a proton-conducting electrolyte offers potential cost and environmental benefits over SOFCs employing an oxygen-ion conducting electrolyte fueled by hydrocarbon fuels. Nitrogen and water are the only chemical products of the direct ammonia SOFCs based on a proton-

conducting solid electrolyte. BCGO is a promising electrolyte material for a direct ammonia fuel cell operating at temperatures of about 600 °C. A $BaCe_{0.8}Gd_{0.2}O_{3-\delta}$ thin film-based single cell has been prepared with the structure Ni-CGO/BCGO/BSCFO-CGO and tested with liquefied ammonia as fuel and oxygen as oxidant. The OCV and maximum power density were 1.12 V and 147 mW cm^{-2}, respectively, at 600 °C. Ammonia can be viewed as an attractive alternative fuel for SOFCs based on proton-conducting electrolytes.

Acknowledgements

References

[1] N.Q. Minh, J. Am. Ceram. Soc. 76 (1993) 563–588.
[2] J.J. Mackenzie, W.H. Avery, Ammonia fuel: the key to hydrogen-based transportation, in: Energy Conversion Engineering Conference, Washington, DC, 1996.
[3] A.S. Chellappa, C.M. Fischer, W.J. Thomson, Appl. Catal. A 227 (2002) 231–240.
[4] A. Wojcik, H. Middleton, I. Damopoulos, J. Van Herle, J. Power Sources 118 (2003) 342–348.
[5] N. Maffei, L. Pelletier, J.P. Charland, A. McFarlan, J. Power Sources 140 (2005) 264–267.
[6] A. McFarlan, L. Pelletier, N. Maffei, J. Electrochem. Soc. 151 (2004) A930–A932.
[7] G.G.M. Fournier, I.W. Cumming, K. Hellgardt, J. Power Sources 162 (2006) 198–206.
[8] Q. Ma, R. Peng, Y. Lin, J. Guo, G. Meng, J. Power Sources 161 (2006) 95–98.
[9] Q. Ma, J. Ma, S. Zhou, R. Yan, J. Guo, G. Meng, J. Power Sources 161 (2007) 86–89.
[10] C.G. Vayenas, R.D. Farr, Science 208 (1980) 593–594.
[11] R.D. Farr, C.G. Vayenas, J. Electrochem. Soc. 127 (1980) 1478–1483.
[12] C. Zou, T.H. Lee, S.J. Song, L. Chen, S.E. Dorris, U. Balachandran, M. Liu, Electrochem, Solid State Lett. 8 (2005) J35.
[13] R. Peng, Y. Wu, L. Yang, Z. Mao, Solid State Ionics 177 (2006), 389-303.
[14] C. Zou, S. Zha, M. Liu, M. Hatano, M. Uchiyama, Adv. Mater. 18 (2006) 3318–3320.
[15] S. Tao, J.T.S. Irvine, Adv. Mater. 18 (2006) 1581–1584.
[16] A. Demin, P. Tsiakaras, Int. J. Hydrogen Energy 26 (2001) 1103–1108.
[17] A.K. Demin, P.E. Tsiakaras, V.A. Sobyanin, S.Yu. Hramova, Solid State Ionics 152–153 (2002) 555–560.
[18] H. Iwahara, Solid State Ionics 28–30 (1988) 573–578.
[19] K.D. Kreuer, Solid State Ionics 97 (1997) 1–15.
[20] K.D. Kreuer, Solid State Ionics 125 (1999) 258–302.
[21] K.D. Kreuer, Annu. Rev. Mater. Res. 33 (2003) 333–359.
[22] C. Xia, M. Liu, J. Am. Ceram. Soc. 84 (2001) 1903–1905.
[23] N. Bonanos, K.S. Knight, B. Ellis, Solid State Ionics 79 (1995) 161–170.
[24] S. Gopalan, A.V. Virkar, J. Electrochem. Soc. 140 (1993) 1060–1065.